Available online at www.sciencedirect.com
ScienceDirect
Journal of Sound and Vibration 301 (2007) 374–390
JOURNAL OF SOUND AND VIBRATION
www.elsevier.com/locate/jsvi

# A generalization of the IDQ method and a DQ-based approach to approximate non-smooth solutions in structural analysis

S. Tomasiello*

*DiSGG - Faculty of Engineering, University of Basilicata, C.da Macchia Romana, 85100 Potenza, Italy*

Received 29 April 2005; received in revised form 12 October 2006; accepted 16 October 2006
Available online 15 December 2006

**Abstract**

In this paper, a new differential quadrature (DQ)-based approach in deducing the discretized equations governing the static and the dynamic problem of the Euler–Bernoulli beam is proposed. These equations, here called generalized, can be written easily, also thanks to a lemma, introduced for the first time, which allow a compact writing of the solution. By means of a careful distribution of the sampling points, the proposed method overcomes the drawback of the element subdivision where load conditions change. This is particularly useful in the analysis of some multi-degree-of-freedom dynamic systems, as it will be shown. The cited distribution and the way of generating it allow to generalize the iterative differential quadrature method, confined, in its initial form, to the two-degree-of-freedom systems.


## 1. Introduction

Recently, the author [1] proposed a method combining the differential quadrature rules with an elements approach. Even if this method is useful for treating easily some structural problems with complex geometry, e.g. frame structures, it does not allow good results without breaking the element where external conditions change, as in the case of discontinuous loads or a load concentrated at certain abscissa. For this reason, one can say that this method does not agree very much with the spirit of the differential quadrature method (DQM), which is to reduce the computational effort as much as possible.

DQM is essentially a collocation method, so it has the disadvantage of choosing in advance a certain number of locations where the equations are satisfied: for many problems in the linear and nonlinear ranges [2–4], the method is sensitive to the choice of sampling points, in spite of a direct substitution of the boundary conditions into governing equations.

In recent years, spectral and pseudospectral collocation methods have captured the interest of the scientific community especially with regard to fluid dynamics and heat transfer [5]. In particular, Legendre and Chebyshev pseudospectral methods are commonly used for the solution of non-periodic differential equations.

*Tel.: +39 971 205060; fax: +39 971 205070.
*E-mail address:* tomasiello@unibas.it.

0022-460X/$ - see front matter © 2006 Elsevier Ltd. All rights reserved.
doi:10.1016/j.jsv.2006.10.008

In some cases, spectral methods and the DQM are identical. For example, when applying these two classes of method to second-order governing equations, the only major difference would be the grid spacing. Generally, high-order systems with more than one kind of boundary condition at each edge arise in mechanics problems. The $\delta$-type grid arrangement represented the first attempt in applying boundary conditions in fourth-order systems [6]. The use of $\delta$-points causes some inconvenience [7] which it is possible to avoid by means of a direct substitution of the boundary conditions into the governing equation [8] at the points immediately neighbouring the boundary. This choice has been proved to be optimal in terms of accuracy and efficiency of the approach [9].

The present work proposes a method which removes the necessity of breaking structural continuity where external conditions change. In the spirit of spectral methods, the proposed approach moves from an integral formulation, but without applying Gaussian integration. The usual quadrature formulas are used, by having assumed as test functions the Lagrange interpolation polynomials. The sampling points have been chosen as the zeros of the first-order derivative of shifted Gegenbauer polynomials of a certain degree $N$ and order $\lambda = -1.4$. To the best knowledge of the author, a similar choice has not been adopted previously.

This choice supplies a logical continuity with respect to the previous work [2,3] of the author introducing the iterative differential quadrature (IDQ) method. In its initial formulation, the method applies differential quadrature rules to discretize the whole space–time domain by using the same distribution of sampling points in each domain direction and by calculating numerical solution over a succession of identical rectangular quadrature grids, giving $M \times N \times N$ points in all, where $N$ is the number of sampling points in one direction and $M$ is the upper limit of the range over which the numerical solution is sought. Thanks to direct substitution of the boundary conditions into governing equations, the dynamic analysis of a two-degree-of-freedom system requires just $N = 6$. Since the method is sensitive to the choice of sampling points, accurate results need a careful distribution generated by a particular rule; by fixing two parameters for this rule, one obtains a distribution which results to be an approximation of the zeros of the first-order derivative of the shifted Gegenbauer polynomial of degree $N = 6$ and order $\lambda = -1.4$, as presented later on.

In this paper, a compact form for the unknown solution of the problem is proposed. This result is achieved independently of the problem and the distribution considered and formalized in a lemma. The discretized equations governing the problem of the Euler–Bernoulli beam have been reformulated in an elegant way, also by using the cited lemma.

The introduction of the so-called generalized loads facilitates the writing of the discretized equations, here indicated as generalized equations, especially for some cases, as for example, the one regarding a nonlinear system with a dynamic concentrated load.

In general, with regard to the space direction, for a certain polynomial degree $N_z$, one can obtain a $(N_z - 4)$-degree-of-freedom system. This represents a generalization of the IDQ method initially proposed.

In order to show the potentialities of the proposed approach, numerical results for some static cases have been tabled and the dynamic analysis of a four-degree-of-freedom nonlinear system has been performed by using $N_z = 8$ points in space direction and $N_t = 6$ points in time direction.

An example of dynamic analysis of a four-degree-of-freedom nonlinear system, but performed by a semi-analytical approach, can be retrieved in Ref. [11].

## 2. The differential quadrature method: an overview

The aim of the method is to approximate the derivative of the solution function at a certain point by means of a weighted linear sum of the function values at all discrete points in the domain of that variable (if one refers to dimensionless variables, as in what follows, the domain is simply (0,1)). In this way, the differential equation governing the problem to be solved is approximated by a set of algebraic equations.

At a point $\zeta = \zeta_i$, the $r$th-order derivative of the function $w(\zeta)$, is given by

$$\left[\frac{\mathrm{d}^r w}{\mathrm{d}\zeta^r}\right]_{\zeta=\zeta_i} = \sum_{j=1}^{N} A_{ij}^{(r)} w_j, \quad i = 1, 2, \ldots, N, \tag{1}$$

where $A_{ij}^{(r)}$ are the weighting coefficients of the $r$th-order derivative.

The off-diagonal terms of the weighting coefficient matrix of the first-order derivative turn out to be:

$$A_{ij}^{(1)} = \frac{\prod_{\substack{v=1 \\ v\neq i}}^{N} (\zeta_i - \zeta_v)}{(\zeta_i - \zeta_j)\prod_{\substack{v=1 \\ v\neq j}}^{N} (\zeta_j - \zeta_v)}, \quad i,j = 1,2,\ldots,N, \quad j \neq i. \tag{2}$$

Eq. (1) can be written easily for a function of two variables as shown in Refs. [3,7].

The off-diagonal terms of the weighting coefficient matrix of the higher-order derivative are obtained through the recurrence relationship:

$$A_{ij}^{(r)} = r\left[A_{ii}^{(r-1)} A_{ij}^{(1)} - \frac{A_{ij}^{(r-1)}}{(\zeta_i - \zeta_j)}\right], \quad i,j = 1,2,\ldots,N, \quad j \neq i, \tag{3}$$

where $2 \leqslant r \leqslant (N-1)$.

The diagonal terms of the weighting coefficient matrix are given by

$$A_{ii}^{(r)} = -\sum_{\substack{v=1 \\ v\neq i}}^{N} A_{iv}^{(r)}, \quad i = 1,2,\ldots,N, \tag{4}$$

where $1 \leqslant r \leqslant (N-1)$.

Assuming the Lagrange interpolated polynomial as test functions, there is no restriction in the choice of the grid coordinates.

Very often the shifted Gauss–Chebyshev–Lobatto (GCL) points are used. For nonlinear problems investigated in Refs. [3,4] the distribution which allows enough accurate results is generated by means of the following rule:

$$\zeta_i = \left(\frac{i-1}{N-1}\right)^{Nb_i/i\sqrt{i}}, \quad i = 1,\ldots,N, \tag{5}$$

where $b_i$ are unknown coefficients to be fixed.

Because of the symmetry of the distribution of sampling points, with $N = 6$, only $b_2$ and $b_3$ need to be fixed.

For $b_2 = 1.4$ and $b_3 = 1.2$, the resulting distribution in the domain $(0,1)$ with $N = 6$ points is

$$(0, 0.008398, 0.28093, 0.71907, 0.991602, 1). \tag{6}$$

This distribution approximates the zeros of the first-order derivative of certain Gegenbauer polynomials.

Gegenbauer polynomials are known to be a particular case of the Jacobi polynomials. An explicit representation of the ultraspherical polynomials of degree $n$ and order $\lambda$, $G_n^{\lambda}(z)$, can be retrieved in Ref. [10].

For $\lambda = \frac{1}{2}$, Gegenbauer polynomials reduce to Legendre polynomials; for $\lambda \to 0$, Gegenbauer polynomials multiplied by $\lambda^{-1}$ differ in the limit from Chebyshev polynomials only by a multiplicative constant.

Calculating the zeros of $G'^{\lambda}_{(N-1)}(\zeta)$ for $\lambda = -1.4$, after shifting this polynomial to cover the domain $(0,1)$, one has

$$(0, 0.008192, 0.284162, 0.715838, 0.991808, 1).$$

In this paper, the sampling points distribution will be generated by calculating the zeros of the shifted $G'^{\lambda}_{(N-1)}(\zeta)$, for $\lambda = -1.4$ and for several values of $N$. As it will be shown afterwards, this distribution, unlike the usual shifted GCL points, ensures results sufficiently accurate for the proposed method.

## 3. The generalized equations

### 3.1. The static case

The proposed approach starts from the formulation of the total potential energy, since the governing equations for static analysis may be derived by minimizing the total potential energy of the beam $E_t$. So, by considering a generic Euler–Bernoulli beam, with regard to the static case and in terms of dimensionless

variables, one has

$$E_t = E_L + E_V, \tag{7}$$

where

$$E_L = \frac{1}{2}\int_0^1 \left(\frac{\mathrm{d}^2 w}{\mathrm{d}\zeta^2}\right)^2 \mathrm{d}\zeta \tag{8}$$

and

$$E_V = -Fw(\zeta_F) \tag{9}$$

in the case of a concentrated load $F$ at the abscissa $\zeta_F$ or

$$E_V = -\int_{\zeta_a}^{\zeta_b} q(\zeta) w(\zeta)\,\mathrm{d}\zeta \tag{10}$$

in the case of a generic distributed load $q(\zeta)$ between the abscissae $\zeta_a$ and $\zeta_b$.

Assuming that in general $\zeta_F$ is not one of the sampling points, it is necessary to explain the dependence on $\zeta$, so the solution function, defined in the domain $(0, 1)$, could be written as proposed in Ref. [1]:

$$w(\zeta) = \mathbf{V}(\zeta)^{\mathrm{T}}\mathbf{d}, \tag{11}$$

where $\mathbf{d}$ is the discretized grid points vector and $\mathbf{V}(\zeta)$ is the shape functions vector whose $j$th component is given by

$$V_j(\zeta) = \delta_{1j} + \sum_{r=1}^{N-1} \frac{A_{1j}^{(r)}}{r!}\zeta^r, \tag{12}$$

where $\delta_{1j}$ is the well-known Kronecker operator; discussion about this result can be retrieved in Ref. [1].

The goal of Ref. [1] was to work in analogy to the FEM formulation; here one wants to overcome the element subdivision where the load condition changes.

For this purpose, a more convenient form for $w(\zeta)$ will be adopted:

$$w(\zeta) = \mathbf{d}^{\mathrm{T}}(\mathbf{A}^{(1)^{\mathrm{T}}}\overline{\mathbf{C}}(\zeta) + \mathbf{B}), \tag{13}$$

where $\mathbf{B}^{\mathrm{T}} = \{1, 0, \ldots, 0\}$, $\mathbf{A}^{(1)}$ is the matrix of the weighting coefficients $A_{ij}^{(1)}$ and $\overline{\mathbf{C}}(\zeta)$ is the vector of the weighting functions $\overline{C}_k(\zeta)$ derived by the Newton–Cotes integration formulas:

$$\overline{C}_k(\zeta) = \int_0^{\zeta} \prod_{\substack{i=1 \\ i\neq k}}^{N} \frac{\zeta - \zeta_i}{\zeta_k - \zeta_i}\,\mathrm{d}\zeta. \tag{14}$$

Eq. (11) has been derived considering that:

$$w(\zeta) - w(0) = \int_0^{\zeta} \mathrm{d}w = \int_0^{\zeta} \frac{\mathrm{d}w}{\mathrm{d}\zeta}\,\mathrm{d}\zeta \tag{15}$$

and by applying the quadrature rules, with the position $w(0) = w_1$:

$$w(\zeta) = w_1 + \sum_{i=1}^{N}\sum_{j=1}^{N} \overline{C}_i(\zeta) A_{ij}^{(1)} w_j. \tag{16}$$

**Lemma.** *For every distribution of sampling points follows that*:

$$\mathbf{V}(\zeta) = \mathbf{A}^{(1)^{\mathrm{T}}}\overline{\mathbf{C}}(\zeta) + \mathbf{B}. \tag{17}$$

**Proof.** If one writes the Lagrange polynomials as follows:

$$L_i = l_{i0} + \sum_{j=1}^{N-1} l_{ij}\zeta^j, \quad i = 1, \ldots, N, \tag{18}$$

where

$$l_{i0} = \begin{cases} 1 & \text{if } i = 1, \\ 0 & \text{if } i \neq 1 \end{cases}$$

for every distribution of sampling points follows that:

$$\sum_{i=1}^{N} l_{ij} = 0, \quad j = 1, \ldots, N-2,$$

$$\sum_{i=1}^{N} l_{ij} \zeta_i^k = \begin{cases} 1 & \text{if } k = j, \\ 0 & \text{if } k \neq j, \end{cases} \tag{19}$$

with $j = 1, \ldots, N-2$ and $k = 1, \ldots, N-2$.

This proves the equivalence (17). □

At this point, it is possible, also by using quadrature rules, to rewrite the terms of the total potential energy as follows:

$$E_V = -F\mathbf{d}^{\mathrm{T}}(\mathbf{A}^{(1)^{\mathrm{T}}}\overline{\mathbf{C}}(\zeta_F) + \mathbf{B}) \tag{20}$$

if a concentrated load $F$ is applied at $\zeta_F$, or

$$E_V = -\sum_{k=1}^{N} C_k^{(a,b)} w_k q_k = -\mathbf{d}^{\mathrm{T}}\mathbf{C}^{(a,b)}\mathbf{q}, \tag{21}$$

if there is a distributed load $q(\zeta)$ between $\zeta_a$ and $\zeta_b$, where $\mathbf{C}^{(a,b)}$ is the diagonal matrix which components are:

$$C_k^{(a,b)} = \int_{\zeta_a}^{\zeta_b} \prod_{\substack{i=1 \\ i \neq k}}^{N} \frac{\zeta - \zeta_i}{\zeta_k - \zeta_i} \, \mathrm{d}\zeta. \tag{22}$$

The elastic energy term is firstly rewritten as

$$E_L = \left[\frac{\mathrm{d}^2 w}{\mathrm{d}\zeta^2}\frac{\mathrm{d}w}{\mathrm{d}\zeta}\right]_0^1 - \left[\frac{\mathrm{d}^3 w}{\mathrm{d}\zeta^3} w\right]_0^1 + \int_0^1 \frac{\mathrm{d}^4 w}{\mathrm{d}\zeta^4} w \, \mathrm{d}\zeta, \tag{23}$$

where the terms in the brackets refer to boundary conditions. In fact, considering also the work done by forces $F_i$ and moments $m_i$ applied in $\zeta = 0$ and 1 and using the quadrature rules, the following equations are obtained:

$$\sum_{j=1}^{N} A_{1j}^{(2)} w_j = m_1, \quad \sum_{j=1}^{N} A_{Nj}^{(2)} w_j = m_N, \tag{24}$$

$$\sum_{j=1}^{N} A_{1j}^{(3)} w_j = F_1, \quad \sum_{j=1}^{N} A_{Nj}^{(2)} w_j = F_N, \tag{25}$$

$$E_L = \frac{1}{2}\sum_{i=1}^{N} C_i w_i \sum_{j=1}^{N} A_{ij}^{(4)} w_j = \frac{1}{2}\mathbf{d}^{\mathrm{T}}\mathbf{C}\mathbf{A}^{(4)}\mathbf{d}, \tag{26}$$

where $\mathbf{C}$ is the diagonal matrix containing the weighting coefficients

$$C_k = \int_0^1 \prod_{\substack{i=1 \\ i \neq k}}^{N} \frac{\zeta - \zeta_i}{\zeta_k - \zeta_i} \, \mathrm{d}\zeta. \tag{27}$$

For the stationarity of the total potential energy, one has

$$\mathbf{C}\mathbf{A}^{(4)}\mathbf{d} = \mathbf{C}^{(a,b)}\mathbf{q} \tag{28}$$

for the case of the distributed load $q(\zeta)$ between $\zeta_a$ and $\zeta_b$, or

$$\mathbf{C}\mathbf{A}^{(4)}\mathbf{d} = F\mathbf{V}(\zeta_F) \tag{29}$$

for the case of the concentrated load $F$ at $\zeta_F$, where $\mathbf{V}(\zeta_F)$ is given by Eq. (17).

Eq. (28) reduces to the usual form

$$\mathbf{A}^{(4)}\mathbf{d} = \mathbf{q} \tag{30}$$

in the case of a distributed load over all the span, since $\mathbf{C} = \mathbf{C}^{(a,b)}$; obviously, if the load is uniformly distributed, the components of the vector $\mathbf{q}$ are equal.

In general, the right side term in Eqs. (30) and (31) can be intended as a generalized load

$$\overline{\mathbf{q}} = \mathbf{D}\mathbf{q}, \tag{31}$$

where $\mathbf{D}$ is a diagonal matrix and $\mathbf{q}$ is a vector, with components equal to $C_k^{(a,b)}$ and $q_k$, respectively, in the case of a distributed load or to $V_k(\zeta_F)$ and $F$ in the case of a concentrated load, with $k = 1, \ldots, N$.

If there is an axial load, one has to consider in Eq. (7) the additional term

$$E_A = -\frac{1}{2}\sigma \int_0^1 \left(\frac{\mathrm{d}w}{\mathrm{d}\zeta}\right)^2 \mathrm{d}\zeta \tag{32}$$

or by integrating by parts

$$E_A = -\frac{1}{2}\sigma \left[\frac{\mathrm{d}w}{\mathrm{d}\zeta} w\right]_0^1 + \frac{1}{2}\sigma \int_0^1 \frac{\mathrm{d}^2 w}{\mathrm{d}\zeta^2} w \,\mathrm{d}\zeta, \tag{33}$$

where the term in the brackets refers to boundary conditions and $\sigma$ is the dimensionless axial load.

So, by applying quadrature rules, one has

$$E_A = \frac{1}{2}\sigma \sum_{i=1}^{N} C_i w_i \sum_{j=1}^{N} A_{ij}^{(2)} w_j = \frac{1}{2}\sigma \mathbf{d}^{\mathrm{T}} \mathbf{C}\mathbf{A}^{(2)}\mathbf{d} \tag{34}$$

and it is possible to write in general

$$\mathbf{C}\mathbf{L}\mathbf{d} = \overline{\mathbf{q}}, \tag{35}$$

where

$$\mathbf{L} = \mathbf{A}^{(4)} + \sigma \mathbf{A}^{(2)}.$$

### 3.2. The dynamic case

For a dynamic system, the distributed inertia forces must be taken into account. Such inertia forces can be written in dimensionless terms as follows:

$$\psi(\zeta, \tau) = -\ddot{w}(\zeta, \tau), \tag{36}$$

where the mass density obviously does not appear explicitly.

With respect to the point having coordinates $(\zeta_i, \tau_j)$, the quadrature rules give

$$\psi(\zeta_i, \tau_j) = -\sum_{l=1}^{N_t} A_{jl}^{(2)} w_{il}. \tag{37}$$

By reasoning in terms of generalized load and by substituting in Eq. (35) the vector $\mathbf{d}$ with the $N_z \times N_t$ matrix $\mathbf{w}$, if there are no other loads, one has

$$\mathbf{w}\mathbf{A}^{(2)^{\mathrm{T}}} + \mathbf{L}\mathbf{w} = \mathbf{0}, \tag{38}$$

since $\mathbf{D} = \mathbf{C}$.

Analogously, one can include the distributed damping forces.

The use of the matrix $\mathbf{w}$ can be justified as follows.

For a generic distributed load one has

$$E_{Vk} = -\int_{\zeta_a}^{\zeta_b} q(\zeta,\tau_k)w(\zeta,\tau_k)\,\mathrm{d}\zeta, \tag{39}$$

i.e. by applying the quadrature rules

$$E_{Vk} = -\sum_{i=1}^{N_z} q_{ik}w_{ik}C_i^{(a,b)} = -\mathbf{w}_k^{\mathrm{T}}\mathbf{C}^{(a,b)}\mathbf{q}_k \tag{40}$$

and in similar way by substituting $w(\zeta)$ with $w(\zeta,\tau_k)$ in Eqs. (23) and (33) one can write:

$$E_{Lk} = \tfrac{1}{2}\mathbf{w}_k^{\mathrm{T}}\mathbf{C}\mathbf{A}^{(4)}\mathbf{w}_k, \tag{41}$$

$$E_{Ak} = \tfrac{1}{2}\sigma\mathbf{w}_k^{\mathrm{T}}\mathbf{C}\mathbf{A}^{(2)}\mathbf{w}_k, \tag{42}$$

where $\mathbf{w}_k$ and $\mathbf{q}_k$ are the vectors corresponding to the $k$th column of the matrices $\mathbf{w}$ and $\mathbf{q}$, respectively.

Since, with respect to the single time $\tau_k$, the stationarity of the total potential energy holds, one can write:

$$\mathbf{C}\mathbf{w}_k{\mathbf{A}^{(2)}}^{\mathrm{T}} + \mathbf{C}\mathbf{L}\mathbf{w}_k = \overline{\mathbf{q}}_k. \tag{43}$$

By rewriting Eq. (43) $N_t$ times for the time sequence $(\tau_1,\tau_2,\ldots,\tau_{N_t})$, one has

$$\mathbf{C}\mathbf{w}{\mathbf{A}^{(2)}}^{\mathrm{T}} + \mathbf{C}\mathbf{L}\mathbf{w} = \overline{\mathbf{q}}, \tag{44}$$

where the generalized load matrix $\overline{\mathbf{q}}$ is given by

$$\overline{\mathbf{q}} = \mathbf{C}^{(a,b)}\mathbf{q} \tag{45}$$

for a distributed load or

$$\overline{\mathbf{q}} = \mathbf{V}(\zeta_F)\mathbf{F}^{\mathrm{T}} \tag{46}$$

for a concentrated load, since for the time coordinate $\tau_k$ it follows that

$$E_{Vk} = -F(\tau_k)w(\zeta_F,\tau_k) = -F_k\mathbf{w}_k^{\mathrm{T}}\mathbf{V}_z(\zeta_F), \tag{47}$$

where

$$w(\zeta_F,\tau_k) = \sum_{j=1}^{N_z} V_{zj}(\zeta_F)w_{jk}, \tag{48}$$

as will be explained in the next section.

## 4. The solution in the space–time domain and the IDQ method

Let $w(\zeta,\tau)$ be the solution to a problem defined over the closed domain $0\leqslant\zeta\leqslant1$, where $\zeta$ and $\tau$ are the space and time dimensionless variables, respectively.

The mathematical formulation of the problem is in terms of partial differential equations to be satisfied over the cited domain, as well as certain conditions to be satisfied at each point of the boundary of the domain.

Where closed-form solutions are not achievable, it is necessary to calculate the approximate solutions, which generally involve domain discretization.

Considering the time domain composed by $M$ subdomains of equal length $\Delta\tau$, the upper limit for the calculus of the solution is $M\Delta\tau$, so in accordance with the IDQ method the solution is computed for $M$ equal subdomain by retrieving each time the initial conditions from the immediately preceding calculus step. The solution over the $k$th interval can be denoted as $w^{[k]}(\zeta,\tau)$, even if in the following equations the index $[k]$ has been omitted for simplicity.

In general, the exact solution in each sub-grid can written as

$$w(\zeta,\tau) = w_a(\zeta,\tau) + r(\zeta,\tau), \tag{49}$$

where $r(\zeta,\tau)$ is the truncation error and

$$w_a(\zeta,\tau) = \mathbf{V}_t^{\mathrm{T}}\mathbf{w}^{\mathrm{T}}\mathbf{V}_z \tag{50}$$

is the approximated solution, with the $N_z \times N_t$ matrix $\mathbf{w}$ containing the values assumed by the function $w(\zeta,\tau)$ in the grid points of the single space–time domain and the shape functions column vectors depending on the space and time variables, respectively, which have the same form (see Eq. (17)).

Accuracy of the solution depends on the function $r(\zeta,\tau)$: for brevity, any consideration about it can be retrieved in Ref. [12].

Now, to construct the global solution, a variable change is first necessary, since in the single subdomain one has to refer to a local coordinate $0 \leqslant \tau \leqslant \Delta\tau$:

$$\tau = \overline{\tau} - (k-1)\Delta\tau, \quad k = 1,\ldots,M.$$

The approximated solution, calculated with the time limit $M\Delta\tau$, can be written as

$$\overline{w}(\zeta,\overline{\tau}) = \sum_{k=1}^{M} u_k(\zeta,\overline{\tau}), \tag{51}$$

where

$$u_k(\zeta,\overline{\tau}) = \begin{cases} w_a^{[k]}(\zeta,\overline{\tau}) & \text{if } (k-1)\Delta\tau \leqslant \overline{\tau} < k\Delta\tau, \\ 0 & \text{otherwise.} \end{cases}$$

It is just the case to observe that, by neglecting the truncation error, Eq. (49) can be also written as

$$w(\zeta,\tau) = \sum_{j=1}^{N_z} V_{zj} \sum_{i=1}^{N_t} V_{ti} w_{ji} \tag{52}$$

in particular, with respect to the sampling points of coordinate $\tau_i$, one has

$$w(\zeta,\tau_i) = \sum_{j=1}^{N_z} V_{zj} w_{ji} = \mathbf{w}_i^{\mathrm{T}}\mathbf{V}_z, \tag{53}$$

since the vector $\mathbf{V}_t$ has all the components equal to zero with exception of the $i$th component which is unit.

Eq. (53), which also appears in the previous section, is substantially equal to Eq. (11), since the vector $\mathbf{w}_i^{\mathrm{T}}$, which is the $i$th column of the matrix $\mathbf{w}^{\mathrm{T}}$, can be read as the vector $\mathbf{d}$ for the static case.

## 5. The model

Consider a slender simply supported beam resting on a hardening nonlinear elastic foundation and which is subjected to a compressive load and to an exciting transverse force $F(\tau) = f\cos\omega\tau$ which is assumed to be applied at the abscissa $\zeta_F$. The foundation is supposed to be defined by the following dimensionless load–displacement relationship: $q(\zeta) = \theta_1 w(\zeta) + \theta_3 w(\zeta)^3$, where $\theta_1$ is the dimensionless linear Winkler foundation stiffness and $\theta_3 > 0$ is the dimensionless hardening nonlinear elastic foundation stiffness.

By considering in the generalized load the contribution of the nonlinear Winkler soil, it is immediate to write for the $k$th interval

$$\mathbf{w}\mathbf{A}^{(2)^{\mathrm{T}}} + \overline{\mathbf{R}}\mathbf{w} + \theta_3\mathbf{w}^3 = \mathbf{C}^{-1}\mathbf{V}(\zeta_F)\mathbf{F}^{\mathrm{T}}, \tag{54}$$

where $\overline{\mathbf{R}} = \mathbf{L} + \theta_1\mathbf{I}$, $\mathbf{w}^3$ is a symbolic notation for the $N_z \times N_t$ matrix containing the $w_{ij}^3$ elements, $\mathbf{F}$ is the vector of $N_t$ components $F_i = f\cos\omega[\tau_i + (k-1)\Delta\tau]$.

By substituting the boundary conditions into Eq. (54), the matrix $\overline{\mathbf{R}}$ reduces to the matrix $\mathbf{R}$ introduced in Ref. [2], to give a system of $(N_z-4)\times N_t$ equations for the generic $k$th interval; in this way, the left side of Eq. (54) can be considered as the matrix form of the Eq. (11) appearing in Ref. [2], even if the time interval length has not been made explicit through the coefficient $\alpha$.

By including in Eq. (54) the initial conditions, the number of equations to be solved for each time step reduces to $(N_z-4)\times(N_t-2)$, as shown in Ref. [2], so one has a reduced matrix $\mathbf{w}_r$ of unknowns.

It is just the case to observe now that all the considerations about the stability and the accuracy of the IDQ method presented in Ref. [3] for a two-degree-of-freedom system can be extended to a multi-degree-of-freedom system. By reading in $\mathbf{w}_r$, as in Ref. [3], the starting value of the row index as 1 instead of 3 and the final value $N_z-4$ instead of $N_z-2$, the equation involved by the stability analysis presented in Ref. [3]

$$\begin{bmatrix}\mathbf{w}_{i+1}\\ \dot{\mathbf{w}}_{i+1}\end{bmatrix}=\mathbf{C}^{(s)}\begin{bmatrix}\mathbf{w}_{i}\\ \dot{\mathbf{w}}_{i}\end{bmatrix} \tag{55}$$

holds with $\mathbf{w}_{i+1}^{\mathrm{T}}=\left[w_{1(i+1)},\ldots,w_{(N_z-4)(i+1)}\right]$ and $\dot{\mathbf{w}}_{i+1}^{\mathrm{T}}=[\dot{w}_{1(i+1)},\ldots,\dot{w}_{(N_z-4)(i+1)}]$ and where

$$\mathbf{C}^{(s)}=\begin{bmatrix}\mathbf{C}_{11}^{(s)} & \mathbf{C}_{12}^{(s)}\\ \mathbf{C}_{21}^{(s)} & \mathbf{C}_{22}^{(s)}\end{bmatrix},$$

with

$$\mathbf{C}_{11}^{(s)}=\mathbf{M}-\frac{A_{11}^{(1)}}{A_{1N_t}^{(1)}}\mathbf{I}_{N_z-4},$$

$$\mathbf{C}_{12}^{(s)}=\mathbf{M}'+\frac{1}{A_{1N_t}^{(1)}}\mathbf{I}_{N_z-4},$$

$$\mathbf{C}_{21}^{(s)}=\mathbf{P}+q_1\mathbf{I}_{N_z-4},$$

$$\mathbf{C}_{22}^{(s)}=\mathbf{P}'+\frac{A_{N_tN_t}^{(1)}}{A_{1N_t}^{(1)}}\mathbf{I}_{N_z-4}.$$

Matrices $\mathbf{M}$, $\mathbf{M}'$, $\mathbf{P}$ and $\mathbf{P}'$ have dimension $N_z-4$ and have the same form shown in Ref. [3] but with

$$\mathbf{B}_{ij}=R_{ij}\mathbf{I}_{N_t-2}+\delta_{ij}\mathbf{S}$$

by having substituted the index $N$ with $N_t$ in all the formulas appearing in Ref. [3] and by considering that the matrices $\mathbf{V}$ and $\mathbf{W}$ in Eqs. (10) and (11) of Ref. [3] can be seen as diagonal matrices where the diagonal elements are the row vectors $(A_{12}^{(1)}\ldots A_{1(N_t-1)}^{(1)})$ and $(q_2\ldots q_{N_t-1})$, respectively, which are repeated $N_z-4$ times.

## 6. Some numerical results

In order to check the behaviour of the method, first the static case has been explored.

Numerical investigations revealed that the proposed method deals with Dirichlet boundary conditions at each edge of the one-dimensional space model, i.e. clamped–clamped, clamped–hinged or simply supported beams show sufficiently accurate results for each load condition, as it will be shown.

Instead, cantilever beams do not ensure good approximation without some precautions; this argument will be treated in a separate paper.

Two kind of load condition have been considered:

(1) a uniformly distributed load between different $\zeta_a$ and $\zeta_b$;
(2) a concentrated load at different abscissas $\zeta_F$.

Table 1
Analytical and numerical results for a clamped–hinged beam with a unit uniformly distributed load on half-span

| | Exact results | $N = 12$ | Error (%) | $N = 17$ (GLC) | Error (%) |
|---|---|---|---|---|---|
| $w(0.5)$ | 0.003092 | 0.003093 | −0.020 | 0.003076 | 0.535 |
| $\phi 1(0.5)$ | −0.004883 | −0.004869 | 0.291 | −0.004844 | 0.785 |
| $\phi 1(1)$ | 0.014323 | 0.014328 | −0.034 | 0.014191 | 0.923 |
| $M(0)$ | −0.054688 | −0.054678 | 0.018 | −0.054952 | −0.483 |
| $M(0.679687)$ | 0.051300 | 0.051494 | −0.378 | 0.051004 | 0.577 |
| $T(0)$ | 0.179687 | 0.185497 | −3.233 | 0.244986 | −36.340 |
| $T(1)$ | −0.320312 | −0.314503 | 1.814 | −0.255016 | 20.385 |

Table 2
Analytical and numerical results for a simply supported beam with a unit uniformly distributed load between $\zeta_a$ and $\zeta_b$

| | Exact results | $N = 12$ | Error (%) | $N = 19$ | Error (%) |
|---|---|---|---|---|---|
| $w(0.5)$ | 0.001427 | 0.001410 | 1.215 | 0.001432 | −0.345 |
| $\phi 1(0)$ | −0.005438 | −0.005359 | 1.439 | −0.005472 | −0.639 |
| $\phi 1(1)$ | 0.003896 | 0.003839 | 1.461 | 0.003900 | −0.111 |
| $T_l$ | 0.075 | 0.075623 | −0.830 | 0.074888 | 0.149 |
| $T_r$ | −0.025 | −0.024791 | 0.837 | −0.024949 | 0.202 |

Table 3
Analytical and numerical results for a clamped–clamped beam with a unit concentrated load at $\zeta_F = 0.8$

| | Exact results | $N = 8$ | Error (%) | $N = 13$ | Error (%) | $N = 21$ | Error (%) |
|---|---|---|---|---|---|---|---|
| $w(0.5)$ | 0.001833 | 0.001854 | −1.145 | 0.001833 | 0.023 | 0.001840 | −0.356 |
| $w(0.8)$ | 0.001365 | 0.001332 | 2.441 | 0.001359 | 0.476 | 0.001371 | −0.412 |
| $\phi(0.8)$ | 0.007680 | 0.007491 | 2.461 | 0.007674 | 0.076 | 0.007734 | −0.703 |
| $M(0)$ | −0.032 | −0.037289 | −16.528 | −0.033158 | −3.619 | −0.031634 | 1.143 |
| $M(1)$ | −0.128 | −0.149829 | −17.054 | −0.124296 | 2.894 | −0.129320 | −1.031 |
| $T_l$ | 0.104 | 0.099485 | 4.341 | 0.108678 | −4.498 | 0.102290 | 1.644 |
| $T_r$ | −0.896 | −0.689963 | 22.995 | −0.815480 | 8.987 | −0.893540 | 0.275 |

Table 4
Analytical and numerical results for a clamped–hinged beam with a unit concentrated load at $\zeta_F = 0.3$

| | Exact results | $N = 12$ | Error (%) | $N = 21$ | Error (%) |
|---|---|---|---|---|---|
| $w(0.3)$ | 0.004079 | 0.004109 | −0.741 | 0.004071 | 0.193 |
| $w(0.5)$ | 0.005344 | 0.005425 | −1.526 | 0.005334 | 0.175 |
| $\phi(0.3)$ | −0.014018 | −0.014209 | −1.366 | −0.013973 | 0.320 |
| $\phi(1)$ | 0.01575 | 0.016399 | −4.118 | 0.015551 | 1.261 |
| $M(0)$ | −0.1785 | −0.186494 | −4.478 | −0.175207 | 1.845 |
| $T_l$ | 0.8785 | 0.790120 | 10.060 | 0.881604 | −0.353 |
| $T_r$ | −0.1215 | −0.124522 | −2.487 | −0.118805 | 2.218 |

Analytical and numerical results, are reported in Tables 1–6 and depicted in Figs. 1 and 2. In tables, $\phi$ is the rotation, $M$ is the bending moment, $T$ the shear stress; the number between brackets is the abscissa value.

Table 5
Analytical and numerical results for a simply supported beam with a unit concentrated load at $\zeta_F = 0.1$

| | Exact results | $N = 8$ | Error (%) | $N = 13$ | Error (%) |
|---|---|---|---|---|---|
| $w(0.1)$ | 0.0027 | 0.002467 | 8.618 | 0.002760 | −2.213 |
| $\phi(0.1)$ | −0.024 | −0.022173 | 7.614 | −0.024507 | −2.114. |
| $\phi(1)$ | 0.0165 | 0.014938 | 9.467 | 0.016768 | −1.622 |
| $T_l$ | 0.9 | 1.037600 | −15.289 | 0.965581 | −7.287 |
| $T_r$ | −0.1 | −0.110450 | −10.450 | −0.110074 | −10.074 |

Table 6
Approximated and exact values of $M_{\max}$ and the $\delta$ shift

| | $\zeta_F$ | $\zeta_a - \zeta_b$ | $N$ | $\delta$ | Approximated | Exact | Error (%) |
|---|---|---|---|---|---|---|---|
| (CC) | 0.8 | – | 13 | 0.0552 | 0.04829 | 0.05120 | 5.686 |
| (CC) | 0.8 | – | 21 | 0.0212 | 0.05084 | 0.05120 | 0.696 |
| (CH) | 0.3 | – | 12 | 0.0633 | 0.08039 | 0.08505 | 5.481 |
| (CH) | 0.3 | – | 21 | 0.0332 | 0.08268 | 0.08505 | 2.789 |
| (CH) | – | 0.2– 0.3 | 12 | 0.0332 | 0.00612 | 0.00612 | 0.029 |
| (SS) | – | 0.2–0.3 | 12 | 0.0140 | 0.01728 | 0.01781 | 2.989 |
| (SS) | – | 0.2–0.3 | 19 | 0.0004 | 0.01782 | 0.01781 | −0.020 |
| (SS) | 0.8 | – | 8 | 0.0563 | 0.16163 | 0.16 | −1.021 |
| (SS) | 0.8 | – | 13 | 0.0387 | 0.15010 | 0.16 | 6.185 |
| (SS) | 0.8 | – | 16 | 0.0292 | 0.15772 | 0.16 | 1.424 |
| (SS) | 0.1 | – | 8 | 0.0889 | 0.07869 | 0.09 | 12.569 |
| (SS) | 0.1 | – | 13 | 0.0426 | 0.08966 | 0.09 | 0.376 |
| (SS) | 0.5 | – | 13 | 0 | 0.23532 | 0.25 | 5.873 |
| (SS) | 0.5 | – | 19 | 0.0049 | 0.24033 | 0.25 | 3.868 |

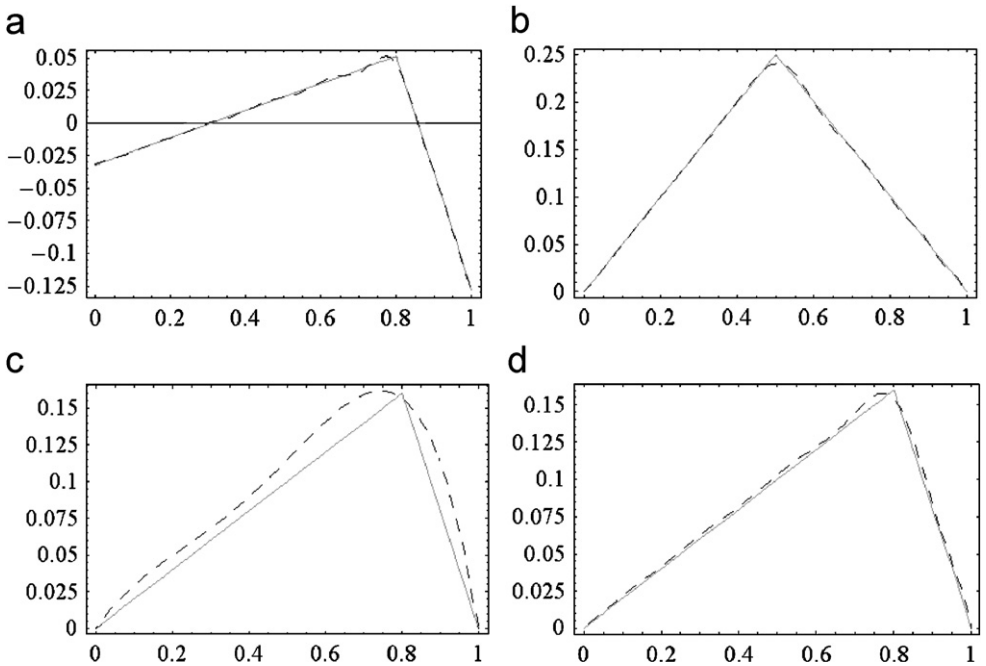


Fig. 1. The bending function in the case of a concentrated load at $\zeta_F = 0.5$ for (b) a simply supported beam with $N = 19$ and at $\zeta_F = 0.8$ for (a) a clamped–clamped beam with $N = 21$, a simply supported beam (c) with $N = 8$, (d) with $N = 16$ (— exact, - - - approximated).

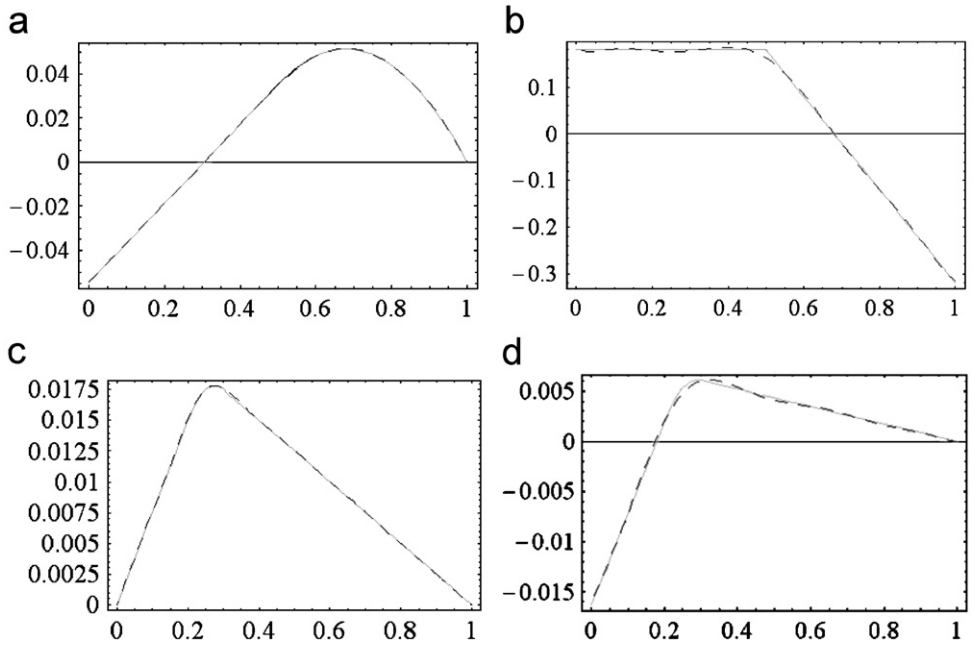


Fig. 2. The bending function (a) and the shear function (b) for a clamped–hinged beam with a unit uniformly distributed load on half-span; the bending function for (c) a simply supported beam ($N = 19$) and for (d) a clamped–hinged beam ($N = 12$) with a unit uniformly distributed load between $\zeta_a = 0.2$ and $\zeta_b = 0.3$ (— exact, - - - approximated).

Table 7
Approximated natural frequencies of a simply supported beam

| $N$ | $\lambda = -1.4$ | Error (%) | $\lambda = 0$ | Error (%) |
|---|---|---|---|---|
| (a) *mode* 1—*exact frequency* 9.869604 | | | | |
| 8 | 9.87089 | −1.303E − 02 | 9.89127 | −2.195E − 01 |
| 12 | 9.86960 | −7.888E − 07 | 9.86961 | −3.049E − 05 |
| 16 | 9.86961 | −6.199E − 06 | 9.86963 | −2.942E − 04 |
| 20 | 9.86090 | 8.821E − 02 | 9.81689 | 5.341E − 01 |
| (b) *mode* 2—*exact frequency* 39.478418 | | | | |
| 8 | 39.34515 | 3.376E − 01 | 40.93409 | −3.687E + 00 |
| 12 | 39.47846 | −1.175E − 04 | 39.48020 | −4.526E − 03 |
| 16 | 39.47842 | −3.846E − 06 | 39.47843 | −2.314E − 05 |
| 20 | 39.48034 | −4.874E − 03 | 39.49352 | −3.824E − 02 |
| (c) *mode* 3—*exact frequency* 88.826439 | | | | |
| 8 | 98.66892 | −1.108E + 01 | 75.49070 | 1.501E + 01 |
| 12 | 88.82130 | 5.788E − 03 | 88.51341 | 3.524E − 01 |
| 16 | 88.82644 | 3.430E − 06 | 88.82573 | 8.010E − 04 |
| 20 | 88.82510 | 1.506E − 03 | 88.80435 | 2.486E − 02 |
| (d) *mode* 4—*exact frequency* 157.9136704 | | | | |
| 8 | 137.31390 | 1.304E + 01 | 99.76259 | 3.682E + 01 |
| 12 | 157.54498 | 2.335E − 01 | 154.36100 | 2.250E + 00 |
| 16 | 157.91335 | 2.035E − 04 | 157.89366 | 1.267E − 02 |
| 20 | 157.91104 | 1.667E − 03 | 157.89754 | 1.021E − 02 |

In Table 1, a comparison between results obtained by the distribution proposed with $\lambda = -1.4$ and those obtainable by the GLC points is presented; generally, the proposed distribution yields sufficiently accurate results with a value of $N$ smaller than the one required by the use of the GLC points.

Table 8
Approximated natural frequencies of a clamped–hinged beam

| $N$ | $\lambda=-1.4$ | Error (%) | $\lambda=0$ | Error (%) |
|---|---|---|---|---|
| (a) *mode* 1—*exact frequency* 15.4182057 | | | | |
| 8 | 15.42207 | −2.509E − 02 | 15.48251 | −4.171E − 01 |
| 12 | 15.41821 | −3.124E − 06 | 15.41823 | −1.298E − 04 |
| 16 | 15.41821 | 4.008E − 06 | 15.41823 | −1.647E − 04 |
| 20 | 15.41370 | 2.925E − 02 | 15.38027 | 2.461E − 01 |
| (b) *mode* 2—*exact frequency* 49.96486203 | | | | |
| 8 | 49.47410 | 9.822E − 01 | 51.22251 | −2.517E + 00 |
| 12 | 49.96484 | 3.937E − 05 | 49.96524 | −7.532E − 04 |
| 16 | 49.96487 | −1.230E − 05 | 49.96487 | −7.710E − 06 |
| 20 | 49.96590 | −2.071E − 03 | 49.97933 | −2.896E − 02 |
| (c) *mode* 3—*exact frequency* 104.248 | | | | |
| 8 | 114.72462 | −1.005E + 01 | 87.60337 | 1.597E + 01 |
| 12 | 104.24526 | 2.633E − 03 | 103.82384 | 4.069E − 01 |
| 16 | 104.24768 | 3.067E − 04 | 104.24645 | 1.484E − 03 |
| 20 | 104.24538 | 2.514E − 03 | 104.21902 | 2.780E − 02 |
| (d) *mode* 4—*exact frequency* 178.27 | | | | |
| 8 | 193.15432 | −8.349E + 00 | 127.58017 | 2.843E + 01 |
| 12 | 177.73329 | 3.011E − 01 | 175.70135 | 1.441E + 00 |
| 16 | 178.26960 | 2.242E − 04 | 178.25959 | 5.841E − 03 |
| 20 | 178.26860 | 7.866E − 04 | 178.25887 | 6.245E − 03 |

Table 9
Approximated natural frequencies of a clamped–clamped beam

| $N$ | $\lambda=-1.4$ | Error (%) | $\lambda=0$ | Error (%) |
|---|---|---|---|---|
| (a) *mode* 1—*exact frequency* 22.3733 | | | | |
| 8 | 22.38083 | −3.364E − 02 | 22.43721 | −2.856E − 01 |
| 12 | 22.37329 | 6.615E − 05 | 22.37331 | −2.414E − 05 |
| 16 | 22.37329 | 5.700E − 05 | 22.37329 | 5.537E − 05 |
| 20 | 22.38423 | −4.884E − 02 | 22.34699 | 1.176E − 01 |
| (b) *mode* 2—*exact frequency* 61.6728 | | | | |
| 8 | 59.76021 | 3.101E + 00 | 63.54792 | −3.040E + 00 |
| 12 | 61.67270 | 1.583E − 04 | 61.67555 | −4.455E − 03 |
| 16 | 61.67282 | −3.422E − 05 | 61.67282 | −3.816E − 05 |
| 20 | 61.68199 | −1.491E − 02 | 61.68410 | −1.833E − 02 |
| (c) *mode* 3—*exact frequency* 120.903 | | | | |
| 8 | 166.00183 | −3.730E + 01 | 114.08716 | 5.637E + 00 |
| 12 | 120.93787 | −2.884E − 02 | 120.69841 | 1.692E − 01 |
| 16 | 120.90340 | −3.279E − 04 | 120.90287 | 1.053E − 04 |
| 20 | 120.91335 | −8.558E − 03 | 120.87725 | 2.130E − 02 |
| (d) *mode* 4—*exact frequency* 199.859 | | | | |
| 8 | 212.34903 | −6.249E + 00 | 137.58706 | 3.116E + 01 |
| 12 | 198.32520 | 7.674E − 01 | 197.36887 | 1.246E + 00 |
| 16 | 199.85922 | −1.090E − 04 | 199.84740 | 5.806E − 03 |
| 20 | 199.86533 | −3.166E − 03 | 199.85996 | −4.781E − 04 |

From tables, one observes that displacements are often well reproduced even for $N=8$, but in order to preserve higher-order derivatives, it is necessary to increase $N$. In some cases, increasing the number of sampling points does not yield better results locally, but improves the result globally over

Table 10
Approximated natural frequencies of a simply supported beam: comparison between errors generated by different numerical methods (8 dof)

| $\lambda = -1.4$ | 4 FE | 2 MQE ($b_2 = 2.2$) |
|---|---|---|
| −7.888E−07 | −2.599E − 02 | −5.447E − 02 |
| −1.175E−04 | −3.946E − 01 | −2.959E − 02 |
| 5.788E−03 | −1.827E + 00 | −3.566E − 01 |
| 2.335E−01 | −1.099E + 01 | −4.232E − 01 |
| −2.899E+00 | −1.291E + 01 | −8.098E + 00 |
| 7.092E+00 | −2.399E + 01 | −4.839E + 01 |
| −6.903E+01 | −3.648E + 01 | −6.415E + 01 |
| −3.645E+01 | −2.716E + 01 | −7.479E + 01 |

Table 11
Approximated natural frequencies of a simply supported beam ($N = 8$, $\sigma = 0.09$)

| $\lambda = -1.4$ | Error (%) | $\lambda = 0$ | Error (%) |
|---|---|---|---|
| 9.87089 | −0.013 | 9.89127 | −0.219 |
| 39.34515 | 0.338 | 40.93409 | −3.687 |
| 98.66892 | −11.081 | 75.49070 | 15.013 |
| 137.31390 | 13.045 | 99.76259 | 36.825 |

the entire domain. In the case of a concentrated load, the step shape characterizing the third-order derivative is not achievable even if the number of sampling points is high, but, considering the frequent disturbance at the ends, the shear on the left-hand and on the right-hand respect to $\zeta_F$ can be expressed as the arithmetical average of the calculated values $T_i$ for $i = 3, \ldots, k_l$ and $i = k_r, \ldots, (N_z - 2)$, respectively, giving in tables $\overline{T}_l$ and $\overline{T}_r$, where $k_l = N_z/2$ and $k_r = ((N_z/2) + 1)$ if $\zeta_F = 0.5$ or, for the other cases, $k_l = M_l - 1$ and $k_r = M_r + 1$, if there is at least one point in each of the resulting intervals, by indicating with $M_l$ and $M_r$ the point closest to $\zeta_F$ from left or from right, respectively.

The maximum value of the second-order derivative can turn out to be slightly shifted with respect to the true abscissa. This shift ($\delta$) in the corresponding bending moment value is reported in Table 6 for a clamped–clamped (CC) beam, for a clamped–hinged (CH) beam and for a simply supported (SS) beam to show how it changes by varying $N$.

Often, especially in the case of a concentrated load, the greater the approximation of $M_{\max}$ the greater the disturbance of the related function (Figs. 1a and b). Besides, a sufficient approximation of $M_{\max}$ does not imply a good approximation for the whole function (Figs. 1c and d). In the same way, a good approximation of the bending function does not imply a good approximation of the displacement and the rotation functions and vice versa (Tables 4 and 5).

In general, the best results are achievable for distributed loads, even if $\zeta_b$ is close to $\zeta_a$ (Fig. 2).

In Tables 7–9 the first four frequencies computed for different beam models with $\sigma = 0$ and for $\lambda = -1.4$ and 0 are reported for increasing values of $N$. Computation with $\lambda = -1.4$ seems to ensure sufficiently accurate results more quickly. An increase in loss of accuracy for higher frequencies however occurs. This drawback is well-known in the elements approach, so in Table 10 a comparison between errors produced by quadrature rules ($\lambda = -1.4, N = 12$) or by an appropriate number of elements for the finite element method and for the modified quadrature element method is proposed for a simply supported beam. In general, the choice $\lambda = -1.4$ seems to be convenient again.

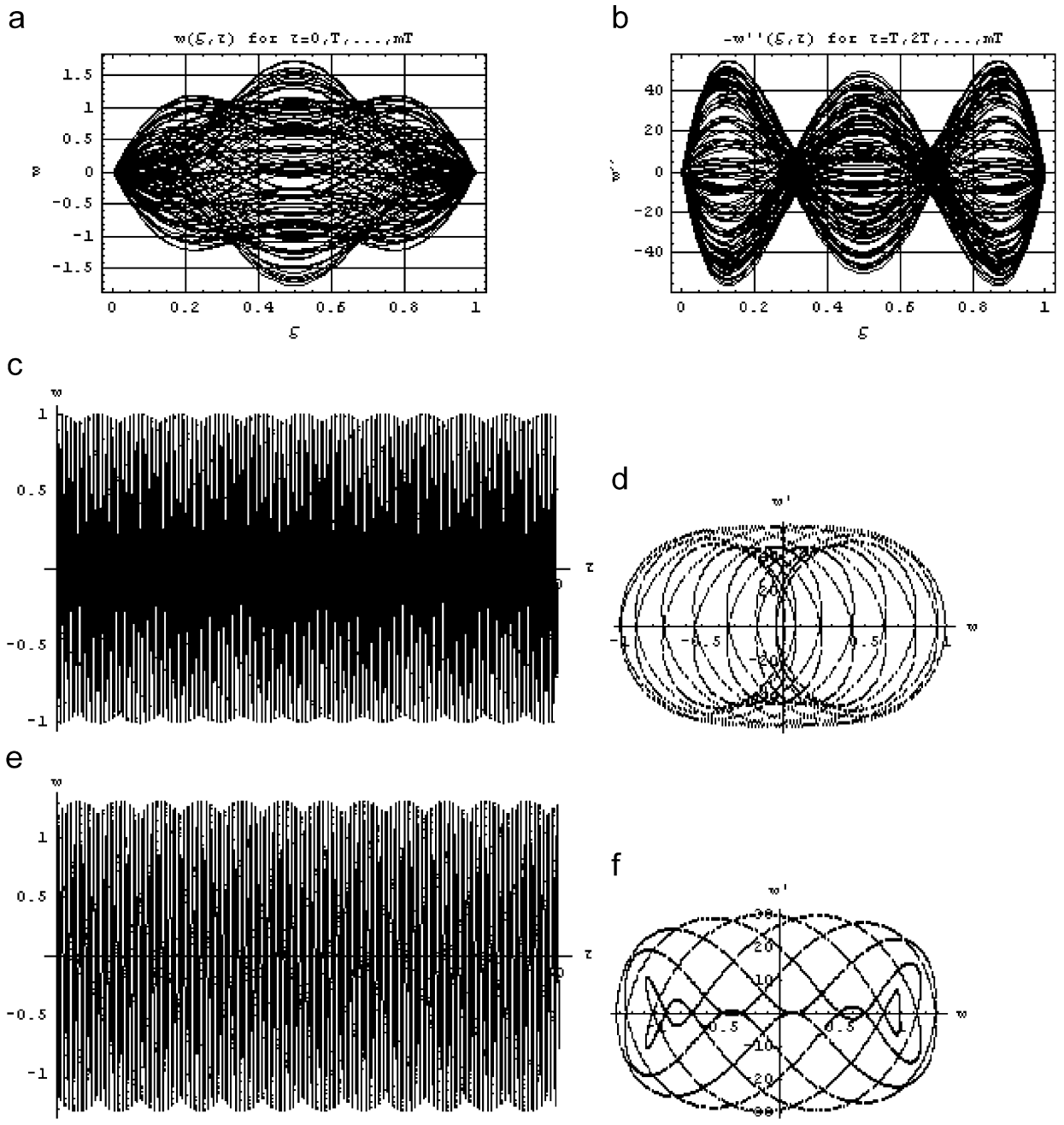


Fig. 3. Simulation of a four-degree-of-freedom system: (a) curves $w(\zeta,\tau)$ and (b) $-w''(\zeta,\tau)$ for $\tau = 0, T, 2T, \ldots, mT$; (c) time history ($0 \leqslant \tau \leqslant 50$) and (d) Poincaré map (2400 points) of the first oscillator; (e) time history ($0 \leqslant \tau \leqslant 50$) and (f) Poincaré map (2400 points) of the second oscillator.

## 7. Simulations

The case $\sigma = 0.09$, $\theta_1 = 0$, $\theta_3 = 100.01$, $f = 1$, $\omega = 300$ is discussed for a four-degree-of-freedom system and, for comparison, for a two-degree-of-freedom system. In Table 11, the natural frequencies (i.e. the square roots of the eigenvalues of the matrix $R$) of the four-degree-of-freedom system are reported for $\lambda = -1.4$ and for $\lambda = 0$.

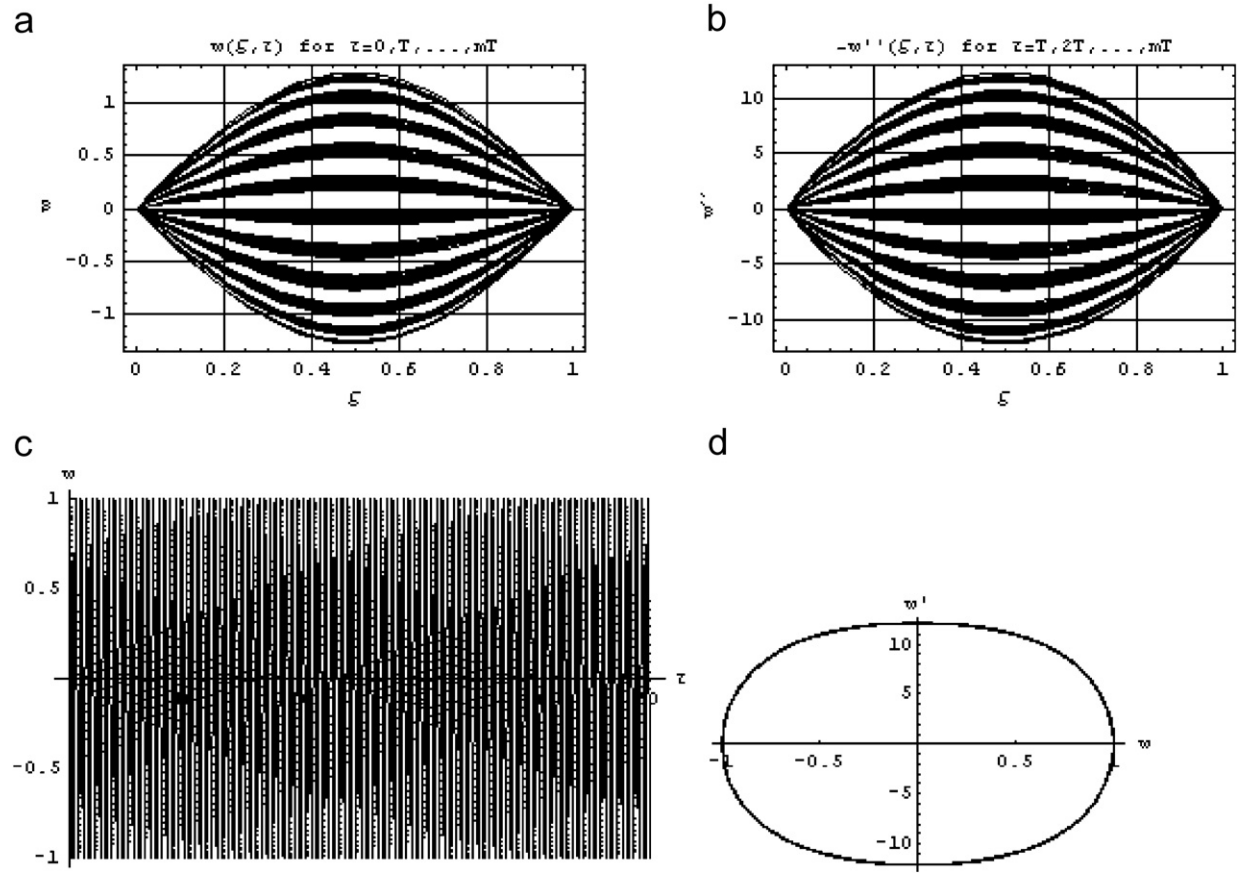


Fig. 4. Simulation of a two-degree-of-freedom system: (a) curves $w(\zeta,\tau)$ and (b) $-w''(\zeta,\tau)$ for $\tau = 0, T, 2T, \ldots, mT$; (c) time history ($0 \leqslant \tau \leqslant 50$) and (d) Poincaré map (2400 points) of the first oscillator.

By considering a free undamped four-degree-of-freedom system with $\sigma = 0.09$ and $\Delta\tau = T_4/5$ one has, being $T_4$ the period of the fourth approximated vibration mode,

$$\mathbf{C}^{(s)} = \begin{bmatrix} 0.602 & 0.248 & -0.108 & 0.059 & 0.862 & 0.087 & -0.039 & 0.022 \\ 0.179 & 0.828 & 0.126 & -0.079 & 0.063 & 0.940 & 0.044 & -0.029 \\ -0.079 & 0.126 & 0.827 & 0.179 & -0.029 & 0.044 & 0.940 & 0.063 \\ 0.059 & -0.108 & 0.248 & 0.602 & 0.022 & -0.039 & 0.087 & 0.862 \\ -0.713 & 0.434 & -0.172 & 0.082 & 0.602 & 0.248 & -0.108 & 0.059 \\ 0.313 & -0.306 & 0.220 & -0.128 & 0.179 & 0.828 & 0.126 & -0.079 \\ -0.128 & 0.220 & -0.306 & 0.313 & -0.079 & 0.126 & 0.827 & 0.179 \\ 0.082 & -0.172 & 0.434 & -0.714 & 0.059 & -0.108 & 0.248 & 0.602 \end{bmatrix},$$

with the conjugate complex eigenvalues

$$\lambda_1 = 0.3090129 \pm 0.9510578I,$$

$$\lambda_2 = 0.6193418 \pm 0.7851214I,$$

$$\lambda_3 = 0.9359706 \pm 0.3520782I,$$

$$\lambda_4 = 0.9959568 \pm 0.0898333I,$$

which have unitary modulus, so the stability condition is satisfied.

The choice $\Delta\tau = T_4/5$ is necessary to ensure the accuracy of the solution, measured through the ratio $T_4/T_4^{\mathrm{ex}}$ which results to be 0.9999965.

For a discretized system with a limited number of degrees of freedom is not very significant to draw the solution in the entire domain, so just the curves $w(\zeta,\tau)$ (Figs. 3a and 4a) and $-w''(\zeta,\tau)$ (Figs. 3b and 4b) for $\tau = 0, T, 2T, \ldots, mT$ are shown, where $T$ is the period of the forcing term. The length of the time interval to compute the solution is assumed to be $\Delta\tau = T/5$. The time histories and the Poincaré map projections onto an appropriate number of planes are shown in Figs. 3 and 4 relatively to a four-degree-of-freedom system and to a two-degree-of-freedom system. As one can observe, the oscillators in both examples have an almost-periodic behaviour, but in the case of a two-degree-of-freedom system, the Poincaré map reveals just one closed loop.

## 8. Conclusions

In this paper, thanks to certain Gegenbauer polynomials, a generalization of the older version of the IDQ method is presented. A lemma, which states a new form for the displacement function, in conjunction with an approximation method to reduce element subdivision and based on differential quadrature rules, allows the so-called generalized equation to be written easily in matrix form. In order to check the approximation method, simple but representative structural examples have been investigated. Finally, a multi-degree-of-freedom system has been successfully simulated by the IDQ method.

## References

[1] C. Franciosi, S. Tomasiello, A modified quadrature element method to perform static analysis of structures, *International Journal of Mechanical Sciences* 46 (2004) 945–959.
[2] S. Tomasiello, Simulating non-linear coupled oscillators by an iterative differential quadrature method, *Journal of Sound and Vibration* 265 (2003) 507–525.
[3] S. Tomasiello, Stability and accuracy of the iterative differential quadrature method, *International Journal for Numerical Methods in Engineering* 58 (2003) 1277–1296.
[4] S. Tomasiello, Differential quadrature method: application to initial-boundary-value problems, *Journal of Sound and Vibration* 218 (4) (1998) 573–585.
[5] C. Canuto, M.Y. Hussaini, A. Quarteroni, T.A. Zang, *Spectral Methods in Fluid Dynamics*, Springer, New York, 1987.
[6] S.K. Jang, C.W. Bert, A.G. Striz, Application of differential quadrature method to deflection and buckling of structural components, *International Journal for Numerical Methods in Engineering* 28 (1989) 561–577.
[7] C.W. Bert, M. Malik, Differential quadrature method in computational mechanics: a review, *Applied Mechanics Review* 49 (1) (1996) 1–28.
[8] C. Shu, H. Du, Implementation of clamped and simply supported boundary conditions in the GDQ free vibration analysis of beams and plates, *International Journal of Solid and Structures* 34 (1997) 819–835.
[9] C. Shu, W. Chen, On optimal selection of interior points for applying discretized boundary conditions in DQ vibration analysis of beams and plates, *Journal of Sound and Vibration* 222 (2) (1999) 239–257.
[10] G. Szegö, *Orthogonal Polynomials*, vol. 32, AMS Colloquium Publications, 1939.
[11] K. Yagasaki, The method of Melnikov for perturbations of multi-degree-of-freedom Hamiltonian systems, *Nonlinearity* 12 (1999) 799–822.
[12] S. Tomasiello, Numerical solutions of the Burgers–Huxley equation by the IDQ method, 2006, in preparation.